DRL No. 77 - DOE/JPL - 955307 - 79/2
Distribution Category UC-63

ANALYSIS OF THE EFFECTS OF IMPURITIES IN SILICON

SECOND QUARTERLY REPORT

FOR PERIOD COVERING

1 MAY 1979 to 31 JULY 1979

BY

J. H. WOHLGEMUTH
W. M. LAFKY
J. H. BURKHOLDER

JPL CONTRACT NO. 955307

SOLAREX CORPORATION
1335 PICCARD DRIVE
ROCKVILLE, MD 20850

DRL No. 77 - DOE/JPL - 955307 - 79/2
Distribution Category UC-63

ANALYSIS OF THE EFFECTS OF IMPURITIES IN SILICON

SECOND QUARTERLY REPORT

FOR PERIOD COVERING

1 MAY 1979 to 31 JULY 1979

BY

J. H. WOHLGEMUTH
W. M. LAFKY
J. H. BURKHOLDER

JPL CONTRACT NO. 955307

SOLAREX CORPORATION
1335 PICCARD DRIVE
ROCKVILLE, MD 20850

"The JPL Low - Cost Solar Array Project is sponsored by the U.S. Department of Energy and forms part of the Solar Photovoltaic Conversion Program to initiate a major effect toward the development of low-cost solar arrays. This work was performed for the Jet Propulsion Laboratory, California Institute of Technology by agreement between NASA and DOE."

ABSTRACT

The purpose of this program is to conduct a solar cell fabrication and analysis program to determine the effects on the resultant solar cell efficiency of impurities intentionally incorporated into silicon. The program will employ "flight-quality" technologies and quality assurance to assure that variations in cell performance are due to the impurities incorporated in the silicon.

During the second program quarter efforts included 1) completion of the processing of verification cells to assure proper process control and to serve as a data base for all future experimental work, 2) study of the dependance of cell performance on crystal orientation to aid in evaluation of the 111 test wafers and 3) completion of the first 5 test runs and analysis of their perfc mance. The verification runs resulted in an average AMO cell efficiency of 12.9% at 25°C (in excess of 15% AMI at 25°C). The average test lot efficiency has varied from 10.6 to 12% at AMO and 25°C. The first 5 test lots have shown a large variation in bulk resistivity (0.2 Ω-cm up to 3.8 Ω-cm) resulting in large variations in lot open circuit voltage (561 mV to 610mV) as would be expected for doping with any active species. The presence of grains boundaries in several wafers had no effect on cell electrical performance. All monitor and control runs to date have cell performance characteristics indistinguishable from the verification runs indicating no contamination.

Table of Contents

1.0 INTRODUCTION

The purpose of this program is to conduct a solar cell fabrication and analysis program to determine the effects on the resultant solar cell efficiency of impurities intentionally incorporated into silicon. A "flight-quality" solar cell process is to be employed with a stringent quality assurance program. The Solarex program has been formulated to assure that:

1) lots do not get misplaced or mixed-up;
2) all processes are well controlled and documented;
3) all equipment is adequately decontaminated after impurity processing;
4) finished cells are analyzed sufficiently to determine the mechanisms limiting performance.

During the second quarter the program effort included 1) completion of the processing of verification cells, 2) study of the dependence of cell performance on crystal orientations and 3) completion of the first five test lots.

Section 2 describes the cell fabrication efforts during this quarter including the cell measurements taken. Section 3 describes the various evaluation parameters employed in the program including a decription of how they are measured and/or calculated and a definition of the parameter. Section 4 contains a description of the analysis performed with the information available to date. Finally, Section 5 describes the activities planned for

the next quarter and contains a revised milestone chart for the program.

2.0 Cell Fabrication

2.1 Verification Cells

The final two verification runs were completed. Summary sheets of the AMO I-V measurements on lot V8 and V10 are included in Appendix A. The average efficiency of the verification lots is 12.9% (AMO at 25°C). Table #1 summarizes the results of the I-V measurements for the six (6) verification runs. Process Evaluation parameters are summarized in Table 2 for the 6 verification lots. This data indicates that the cell processing is consistent from lot to lot. This data base will be used as a baseline for the experimental runs.

2.2 Crystal Orientation Dependence

The initial process sequence was developed using a NaOH etch designed for 100 silicon. Upon completion of the verification run it was discovered that the test wafers were all from ingots grown from 111 seeds. Therefore the etch procedure had to be modified, since NaOH etches 111 silicon too slowly. The etch is now being performed in CP26 consisting of 5 parts HNO_3, 3 parts HF and 6 parts acetic acid. Because the verification lots were run using 100 silicon with a NaOH etch, a set of experiments were run to determine the comparative performance of 100-NaOH and 111-CP silicon solar cells. Table 3 summarizes the results of these runs. All the measurements are within two standard deviations except the red component of the current, which is statistically lower for the 111 cells.

TABLE I

SUMMARY OF VERIFICATION LOTS V-4,-5,-6,-8,-10

Red = Corning #2408
Blue = Corning #9788

Lot #	Isc mA	Voc mV	Pmax. mW	Imp mA	Vmp mV	Isc Blue mA	Isc Red mA	Fill Factor %
V-4 (33 cells)								
AVG.	148.9	595.7	69.0	139.1	496.0	39.9	82.5	77.8
σ	1.72	1.95	2.00	3.44	7.43	1.57	1.30	--
Coef. Var.	.012	.003	.029	.025	.015	.039	.016	--
V-5 (36 cells)								
AVG.	149.1	595.6	68.9	138.8	496.1	39.2	83.3	77.6
σ	1.46	1.15	2.38	4.58	10.85	1.12	.94	--
Coef. Var.	.010	.002	.035	.033	.022	.029	.011	--
V-6 (34 cells)								
AVG.	152.4	597.7	71.1	143.1	497.6	40.7	83.2	78.2
σ	1.10	1.53	1.34	2.41	5.10	1.34	.99	--
Coef. Var.	.007	.003	.019	.017	.010	.033	.012	--
V-7 (27 cells)								
AVG.	149.3	595.7	69.6	140.0	496.9	37.6	84.7	78.2
σ	1.70	2.06	1.33	2.67	4.83	1.39	1.06	--
Coef. Var.	.011	.003	.019	.019	.010	.037	.013	--
V-8 (38 cells)								
AVG.	151.4	594.0	69.9	141.6	506.3	37.4	85.5	79.7
σ	1.88	2.17	2.21	3.92	11.27	2.62	1.70	--
Coef. Var.	.012	.004	.032	.028	.022	.070	.020	--
V-10 (37 cells)								
AVG.	151.3	591.5	70.2	141.2	496.3	38.2	85.0	78.3
σ	1.63	1.97	1.29	1.98	4.15	1.05	1.80	--
Coef. Var.	.011	.003	.018	.014	.008	.027	.021	--
Σ6 Lots								
AVG.	150.4	595.0	69.8	140.6	498.2	38.8	84.0	78.3
σ	1.48	2.09	.818	1.64	4.01	1.32	1.19	.74
Coef. Var.	.010	.004	.012	.012	.008	.034	.014	.009

TABLE 2

PROCESS EVALUATION MEASUREMENT

Lot No.	Pmax mA	Photon Abs.Effic. α in %	Quantum Yield		Carriers Collected Per Absb. Photon	Junction Cap. MF	Junction Cond. MΩ	R_{series} Ω	R_{shunt} KΩ	Diode Factor n	Io mA
			λ max. μ	% Q Y at λmax							
V-4	69.0	.91	.6	89	.82	.115	.03	.074	50.8	1.02	$3X1^{-8}$
V-5	68.9	.91	.6	93	.84	.112	2.96	.046	0.345	1.05	$3X10^{-8}$
V-6	71.1	.91	.6	91	.83	.116	.24	.063	4.71	1.05	$3X10^{-8}$
V-7	69.6	.91	.6	92	.84	.093	.29	.089	11.6	1.02	$3X10^{-8}$
V-8	69.9	.91	.65	93	.85	.117	.47	.099	1.56	1.10	$5X10^{-8}$
V-10	70.2	.92	.65	90	.81	.111	.35	.092	4.96	1.10	$5X10^{-8}$

TABLE 3 COMPARISON OF 100 AND 111 CELL PERFORMANCE

Description	Isc mA	Voc mV	Pmax. mW	Imp mA	Vmp mV	Isc Blue mA	Isc Red mA
CP-111 Avg.	148.1	593.4	69.1	139.2	496.4	38.4	80.1
Ver. Lots Avg.	150.4	595.0	69.8	140.6	498.2	38.8	84.0
σ	1.48	2.09	.818	1.64	4.01	1.32	1.19
Coef. Var.	.01	.004	.012	.008	.034	.014	.009

Because of the similarity in cell performance and the presence of a baseline control lot among the test wafers, only 100-NaOH etched wafers will be used to make the control and monitor cells.

2.3 Monitor and Control Runs

To assure consistent cell processing and successful decontamination of the equipment, a monitor lot is run before each test lot and control silicon is run with the test wafers. The first five (5) monitor and control lots have exhibited performance indistinguishable from the verification lots.

2.4 Test Runs

To date the first five test lots have been processed. Appendix B includes a tabluation of the AMO I-V measurements made on Test Lots 1,2,3,4 and 5. Table 4 summarizes the results of the I-V measurements on these lots. Table 5 presents the same data as a fraction of the verification values. Table 6 summarizes the process evaluation measurements for the first 5 test and control lots.

The following observations have been made:

1) Test lot 1 contained single crystal seed wafers and polycrystalline center and tang wafers. There was no noticeable difference in performance between the single crystal and polycrystalline cells.

TABLE 4

PERFORMANCE OF FIRST FIVE EXPERIMENTAL LOTS

Lot	Isc mA	Voc mV	Pmax mW	Imp mA	Vmp mV	Isc Blue mA	Isc Red mA	Fill Factor %
Verif. (6 Lot AVG)	150.4	595.0	69.8	140.6	498.2	38.8	84.0	78.3
E-1 Test Cells	143.5	573.3	60.8	128.5	472.5	36.3	80.5	73.8
E-2 Test Cells	144.2	578.2	64.7	134.5	480.8	40.5	76.3	77.6
E-3 Test	134.2	610.1	59.3	114.8	515.9	37.0	71.4	72.4
E-4 Test	138.9	606.5	64.0	125.5	510.0	38.2	72.9	76.0
E-5 Test	134.6	561.2	57.6	121.8	472.0	37.9	69.5	76.3

TABLE 5

PERFORMANCE OF FIRST FIVE EXPERIMENTAL LOTS

Lot	Isc Exp. / Isc Ver.	Voc Exp. / Voc Ver.	Pmax. Exp. / Pmax Ver.	Imp Exp. / Imp Ver.	Vmp Exp. / Vmp Ver.	Isc Blue Exp. / Isc Blue Ver.	Isc Red Exp. / Isc Red Ver.
E1	.95	.96	.87	.91	.95	.94	.96
E2	.96	.97	.93	.96	.97	1.04	.91
E3	.89	1.03	.85	.82	1.04	.95	.85
E4	.92	1.02	.92	.89	1.02	.98	.87
E5	.89	.94	.83	.87	.95	.98	.83

TABLE 6

TEST LOT PROCESS EVALUATION

Lot	Pmax mW	Absorption Efficiency %	Quantum Yield λ max. μ	Quantum Yield % Q Y at λmax	Carriers Collected per Absb. Photon	Junction Cap. μF	Junction Cond. MU	R_{series} Ω Avg.	R_{shunt} Ω Median	Diode Factor	Io MA x10^{-6}
Verification lot AVG	69.8	91	0.62	91	0.83	0.111	0.72	0.74	5,000	1.05	3.78
E-1 Control (100)	69.6	91	0.65	83	0.83	0.111	0.10	0.083	7,140	1.03	3.0
E-1 Test	60.7	88	0.65	85	0.79	0.063	1.43	0.19	450	1.47	1000.
E-2 Control, (100)	68.6	91	0.60	89	0.82	0.107	0.01	0.115	9,000	1.02	3.2
E-2 Test	64.3	87	0.65	87	0.85	0.086	0.40	0.092	1,200	1.05	9.3
E-3 Control (100)	68.9	91	0.65	91	0.84	0.106	0.04	0.048	10,636	1.01	2.0
E-3 Test	59.3	88	0.65	84	0.77	0.344	11.86	0.040	295	1.42	2000.
E-4 Control (100)	69.4	90	0.65	85	0.80	0.103	0.07	0.057	1,681	1.08	9.0
E-4 Test	64.0	89	0.60	83	0.79	0.341	0.71	0.050	184	1.18	8.0
E-5 Control (100)	69.3	94	0.65	92	0.86	0.103	0.13	0.081	3,255	1.11	9.0
E-5 Test	55.3	83	0.60	87	0.78	0.082	4.44	0.091	246	1.13	40.

2) The higher open circuit voltage of lots 3 and 4 is consistent with their measured bulk resistivity (0.2Ω-cm) and confirmed by the junction capacitance measurements.

3) The lower open circuit voltage of lots 1,2 and 5 is consistent with their higher bulk resistivity (3.0 to 5.0Ω-cm).

4) There is no statistical difference between cells made from the seed, center or tang end of each ingot.

3.0 Definition of Evaluation Parameters

Various cell parameters are measured on sample cells of each lot in order to assure consistent processing and to provide additional information on cell behavior. The following sections describe the parameters including how they are measured and/or calculated and how they relate to physical mechanisms in the cell.

3.1 Absorption Efficiency

This value represents the fraction of incoming photons incident on the cell surface that actually enter the cell, as a function of wavelength.

The intensity of a reflected light beam is measured (versus wavelength) in an integrating sphere spectrophotometer with a Beckman DK-2 monochromator as the light source. The corrected reflectance represents the intensity ratio of the reflected beam to the incoming beam, thus normalizing for variations in the incoming light beam. Utilizing published data, the number of photons per unit area absorbed into the cell is computed for each 0.1 u band width between 0.4 μ to 1.0 μ. The ratio of the number of photons absorbed to the number of incoming photons, integrated for the six band widths, is the absorption efficiency.

This value is used to check the quality of the anti-reflector coating applied to the cell. Consistency of this parameter assures that the optical coupling to the cells is the same.

3.2 Quantum Yield

This value represents the ratio of carriers collected to the number of incoming photons per a unit area as a function of wavelength.

A light beam is passed through a monochromator and alternately impinges on a defined unit area on the test solar cell and on a calibrated Eppley thermopile. The measured cell current is converted into the number of carriers collected. The current in the calibrated thermopile is used to find the number of incident photons. This ratio represents the cells efficiency of converting photons into carriers and collecting these carriers. Taking these measurements as a function of wavelength results on a curve of quantum efficiency over the band width of solar radiation. The wavelength at which the maximum quantum efficiency occurs and the percent efficiency at this point are listed in the process evaluation table. An independent measurement of the shunt resistance enables one to correct for any internal shunting of carriers. However, other cell parameters such as short carrier lifetime and reflection of photons from the cell surface all contribute to a reduced quantum yield.

3.3 Carriers Collected per Absorbed Photon

No independent measurement is required as this parameter equals the ratio of quantum yield to absorptivity summed over the entire solar spectrum. This ratio represents a modified quantum yield in that the effect of photon reflection is removed. Thus one measures the collection efficiency of the photons that enter the silicon.

3.4 Junction Capacitance

The junction capacitance is the capacitance across the depletion region of the junction. It is measured with a Capitance Bridge using an ac signal with no dc voltage across

the junction.

For lightly doped p type bulk and a heavily doped n type junction, the step-junction approximation is appropriate. The depletion region exists primarily on the p side to a width adequate to ionize enough acceptors to equal the number of ionized donors in a very narrow segment of the heavily doped n side. The width of the depletion layer is fixed by the voltage developed between the opposing two layers of charge; 1) the electrons on the p side of the depletion layer and; 2) the holes on the n side of the depletion layer.

The depletion region is in effect a parallel plate capacitor whose interplate spacing is proportional to the relative doping levels of the p and n sides.

3.5 Junction Conductance

This is a measurement of the cell leakage current and is read directly by the capacitance bridge as a resistance in parallel with the junction capacitor.

3.6 Series and Shunt Resistance

A solar cell is not a perfect diode. Each real cell has an effective resistance in series with the junction and a shunt resistance in parallel with the junction. The series resistance includes components from contact resistance in both the front and the back contacts, the resistance of the bulk silicon and the sheet resistance in the diffused region. The shunt resistance may be caused by surface leakage along the edge of the cell, by

diffusion down dislocations or by metallization paths across the junction.

The idealized cell equation is given by

(1) $I = I_L - I_{01} \left(\exp \left(\frac{qV}{nkT} - 1\right)\right) - I_{02} \left(\exp \left(\frac{qV}{kT} - 1\right)\right)$

where I = current collected from the cell

I_L = light generated current

J_{01} = reverse diode saturation current of space change region

I_{02} = reverse diode saturation current of quasi-neutral region

$\frac{kT}{q}$ = thermal voltage

n = diode factor

V = voltage across the junction

If you take into account the series resistance and shunt resistance terms this equation becomes:

(2) $I + \frac{V+IRs}{Rsh} = I_L - I_{01} \left(\exp \frac{q}{nkT} (V-IRs) - 1\right) - I_{02} \left(\exp \frac{q}{kT}(V-IR_s) - 1\right)$

where Rs = series resistance

Rsh = short resistance

The series resistance is derived from a comparison of two I-V curves for a cell at two distinct light levels, I_1 and I_2 where $I_2 \approx 2I_1$. A point is chosen on each I-V curve at an arbitrary level set 30 mA below the I_{SC} at each light level. The slope of a straight line connecting these two points is the series resistance.

The shunt resistance is calculated by measuring the reverse current of the cell in the dark while maintaining 0.1 volts across the cell. The ratio of voltage to the current is then used as a measure of the shunt resistance. This is only an approximate

value because the presence of a shunting diode may affect the measured current. However we are only using it as indication of the junction quality so that a small value of this measured ratio indicates a problem in cell junction due to either a resistive or diode shunt.

3.7 Diode Factor and Reverse Saturation Current

The diode factor and the reverse diode saturation current can be attained from either the static dark I-V characteristic or from the static I_{SC} - V_{oc} (photo-current versus photo-voltage) response to various levels of illumination. The current in both cases has two components-one originating from recombination within the spare charge region-and the other from recombination in the quasi-neutral region.[1] The first exponential term in equation 2 is the component arising from the space charge region, with an effective diode factor of n and a diode saturation current of I_{01}. The second exponential term is the current component arising from the quasi-neutral regions with a diode factor of unity and a diode saturation current of I_{02}. The parameters I_{01}, I_{02} and n are determined using a method previosly described in the literature[2,3,4].

The problem with this exact technique is the complicated relationship between the two diodes and the lack of any convenient parameter to determine in what regime the cell is actually operating. In other words, is the space charge diode or quasi-neutral diode dominating at the peak power point. To answer this question in simple manner, we have assumed the presence of only one diode operating at the maximum power point. The equation for I would

then become:

$$(3)\quad I + \frac{V+IRs}{R_{sh}} = I_L - I_o \left(\exp \frac{q}{nkT} (V-IRs) - 1\right).$$

I_o and n are then calculated from the intercept and slope of the curve drawn target to the I_{SC} vs V_{oc} curve at the voltage of maximum power. If the value of n is appreciably larger than 1, the space charge diode or a resistive shunt is affecting the cell peak power. Large values of I_o also indicate a lowering of the peak power due to diode or resistive shunting.

4.0 Analysis

4.1 Impurity Content

The wafers supplied to Solarex by JPL were grown by the Westinghouse/Dow Corning team under JPL Contract Number JPL-954333. The growth process and impurity contents are given in the Tenth and Eleventh Quarterly Reports[5,6] for this program. Table #7 summarizes the identity and properties of these test wafers.

4.2 Statistical Methods

The statistical methods used in the following analysis are based on the General Linear Model; more specifically, the Multiple Linear Regression technique(MLR). Briefly, the MLR approach is a univariate technique which has the capability of adapting to a variety of commonly used statistical methods. Briefly, MLR analogs of the Students T and analysis of variance and covariance were used.

The MLR program (Linex.For) used in this study was adapted by the authors (JHB) from two earlier versions (Linear.For & LingrF.For) originally implemented tc run in a batch oriented main frame, computer. The present version was redesigned to function interactively on Solarex's PDP 11/03V Computer.

The principal avenue of investigation was the identification of statistical differences between the varification lots and experimental lots given by the following hypotheses:

H_1: Does a statistical difference exist between varification groups vs individual experiments groups

Table #7

IDENTITY OF TEST WAFERS

Experimental Lot #	Ingot #	Type of Growth	Impurity	Best Estimate of Concentration 10^{15} atoms/cc	Bulk Lifetime (as grown) μsec	Bulk Resistivity Ω-cm	Notes
1	W-086	CZ	C	200-400	3.06	3.5-4.0	Polycrystalline
2	W-087	CZ	Ca	?	2.81	3.4-3.8	
3	W-088	CZ	Cr	0.5	0.01	0.18-0.2	
4	W-089	CZ	Cu	2.0	2.37	0.19-0.21	
5	W-095	FZ	Mn	0.63	0.343	4.2-4.9	fast growth

All Data from Westinghouse-Dow Corning - 11^{th} Quarterly Report Reference 6.

for the dependent measures of a) I_{sc}, b) Vo_c, c) P_{max}, d) V_{max}, e) I_{max}, f) I_{sc}Red, h) bulk resistivity, i) sheet resistance, j) buss pattern resistance.

- elements a) to g) = Performance dependent, variable
- elements h) to j) = Process dependent variables

Model 1:

$$y = b_o U + b_1 X_1^* + b_2 X_2^* + E$$

(Full Model)

$$y = b_o U + E$$

(Residual Model)

* Dummy binary vectors identify membership to treatment.

H_2: Does a statistical difference exist between varification groups vs individual experimental groups performance dependent variables over and above the effects of process dependent variables (covariates)

Model 2:

$$y = b_o U + b_1 X_1 + b_2 X_2 + \left[b_n X_n \right] + E$$

(Full Model)

$$y = b_o U + \left[b_n X_n \right] + E$$

(Residual Model)

where: $\left[b_n X_n \right]$ are covariate(s)

In addition to this, a correlation matrix was generated for all varification and experimental data sets together for

all dependent variables.

The subsequent analysis employed a relatively large N size. As a result the statistical power is very high making the establishment of a conventional statistical significance level, such as $\alpha = .05$ or .01, to be of little value. For this reason it was deemed appropriate to dispose with convention and establish another criteria for significance. Because exact probabilities were calculated it was assumed sufficient and advantageous to regard as significant the relative changes in exact probabilities relative to explaining the underlying physical phenomena investigated in this study.

4.3 Correlations

The initial statistical analysis involved the generation of a correlation matrix using the data from all of the verification and experimental cells. The light I-V parameters, bulk resistivity, sheet resistance and buss resistance are all correlated with each other as shown in Table 8. The information in This table suggests the following observations:

1) There is a high positive correlation between short circuit current(I_{sc}), and maximum power (P_{max}), indicating that the current is an important determining factor for cell power.
2) There is no correlation between the open circuit voltage (V_{oc}) and, maximum power(P_{max}) indicating that when restricted to identical cell processing, there is no relation between open circuit voltage and peak power.

Table 8

PEIRSON PRODUCT MOMENT CORRELATION MATRIX OF

PERFORMANCE & PROCESSING VARIABLES*

	I_{sc}	V_{oc}	P_{MAX}	I_{mp}	V_{mp}	$I_{sc}b$	$I_{sc}R$	blk-Res	Sht-Res	buss-Res
I_{sc}	1.0									
V_{oc}	0.283	1.0								
P_{MAX}	0.804	0.424	1.0							
I_{mp}	0.853	0.201	0.930	1.0						
V_{mp}	0.134	0.704	0.453	0.20	1.0					
I_{sc}blue	0.247	0.090	0.256	0.295	-0.074	1.0				
I_{sc}red	0.901	0.232	0.718	0.756	0.165	-0.065	1.0			
blk-Res	-0.034	-0.849	-0.109	0.084	-0.522	0.016	-0.077	1.0		
Sht-Res	0.484	-0.057	0.327	0.427	0.109	0.082	0.439	0.1092	1.0	
Buss-Res	0.502	-0.049	0.343	0.411	0.035	0.032	0.434	-0.071	0.494	1.0

*MATRIX OF CORRELATIONS CONTAINS ALL VARIFICATION AND EXPERIMENTAL DATA SETS

$r \leq 0.138 + p > .01$ for N = 200

3) There is a very high positive correlation between I_{sc} and I_{mp} and between V_{oc} and V_{mp}, showing that it is cell collection efficiency not fill factor that significantly affect cell performance. (Fill factor variations are small due to proper design and fabrication of the cells).

4) There is a high positive correlation between I_{sc} and I_{sc} red, while I_{sc} blue is not correlated with any other variables. The I_{sc} red values vary considerably from lot to lot, reflecting bulk degradation due to impurity content. The I_{sc} blue values are quite constant from lot to lot indicating good control over the cell processing.

5) There is a high negative correlation between open circuit voltage (V_{oc}), and bulk resistivity corresponding to the theoretical dependence of cell voltage on bulk resistivity.

6) There is a mild correlation between I_{sc}, I_{mp} and I_{sc} red with the processing variables sheet resistance and buss resistance. The mild negative correlation between buss resistance and current could be as a result of thicker buss plating leading to a large fraction of the cell area being covered by metallization. The correlation of sheet resistance to bulk current and buss resistance is unexplained at this time. There is no correlation between blue current and sheet resistance so the effect is not the typical dependence of short wavelength response on depth of diffusion.

4.4 Analysis of Verification VS Experimental Groups

The I-V measurement of each test lot were compared individually with the verification cells and the effect of bulk resistivity, sheet resistance and buss resistance factored out. Rather than providing a large number of ANOVA Tables[7], we have elected to present only an evaluation of the most salient results of this analysis. Except for I_{SC} blue, all other I-V parameters realized highly significant treatment group differences ranging from $P = 1.6 \times 10^{-4}$ to $P = 1. \times 10^{-10}$ probability. The discussion to follow presents the analysis in two ways; a) evaluation of treatment differences after covariation and b) evaluation of change in statistical characteristics as a function before/after covariation.

Such general observations can be made. Much of the variation in open circuit voltage was due to the variation in bulk resistivity. Likewise some of the variation in current was due to the bulk resistivity and to a lesser extent due to the cell coverage.

The following sections describe the type of degradation observed for each experimental group.

1. E-1 has a decrease in voltage due in part to a slightly higher bulk resistivity than the verification cells. The blue current is not statistically different from the verification lots. The major degradation is in the bulk or red current, indicating a decrease in bulk lifetime. Also there is a decrease in fill factor due to resistive and diode shunting suggesting the presence of a high concentration of carbon near the junction.

2. E-2 exhibits a decrease in open circuit voltage mainly due to a higher bulk resistivity. This lot had a higher blue current component than the verification lots. Once again the major degradation occurred for the bulk red current, again indicating a decrease in bulk lifetime. The fill factor of lot E-2 is nearly equal to the average of the verification lots. The junction diode is well behaved for these test cells, being indistinguishable from the verification cell diodes. Therefore it appears that calcium does not degrade junction performance.

3. E-3 exhibited a significantly higher open cirucuit voltage, that was almost entirely attributable to the lower bulk resistivity. This lot also exhibited a lower short circuit current. However, when the effect of the covariates were factored out neither the short circuit current nor the bulk current were statistically different indicating that the chrome has not significantly degraded the bulk lifetime. The blue current is slightly less on the test cells and the covariates analysis indicates that this difference is not due to the covariates. Finally the test cells exhibited lower fill factors due to both resistive and diode shunting. These results indicate that the chrome probably migrates out of the bulk into the n^+ region of the cell.

4. E-4 once again exhibited a higher open circuit voltage and lower current attributable to the lower bulk resistivity of the test wafers. Indeed when the affect of the covariates is factored out, there appears to be no statistical difference between the maximum power of the test cells and the maximum power of the verification cells. Correspondingly, the fill factor is also nearly the same. At this level of doping the copper does not appreciably effect the cell performance.

5. E-5 exhibits a lower open circuit voltage than the verification cells, This is partially due to a higher bulk resistivity. The major degradation is due to red or bulk current. This loss in current is due to a decrease in bulk lifetime caused by the manganese. The fill factor of this lot is nearly as high as for the verification lots, however several cells show appreciable resistive shunts, while the majority have excellent diode characteristics. Since none of the monitor or control cells have shown is shunting, we feel it is a result of impurity level. At present we do not know why it occurs in some but not all cells.

The statistical analysis will continue throughout the program. As additional data is obtained the various statistical calculations will be repeated to assure optimum accuracy. It now appears that time permitting, verification cells should be fabricated using silicon with a variety of resistivities in order to further analyze the effect of bulk resitivity on cell performance as opposed to the effect of impurity concentration on cell performance.

5.0 Planned Activities

During the coming months the processing of experimental and monitor lots will continue. A total of 45 different impurity lots are scheduled with an average of approximately 7 lots per month planned for the remainder of the program. A revised program milestone chart is shown in Figure 5-1.

FIGURE 5-1 PROGRAM PLAN

MILESTONE CHART

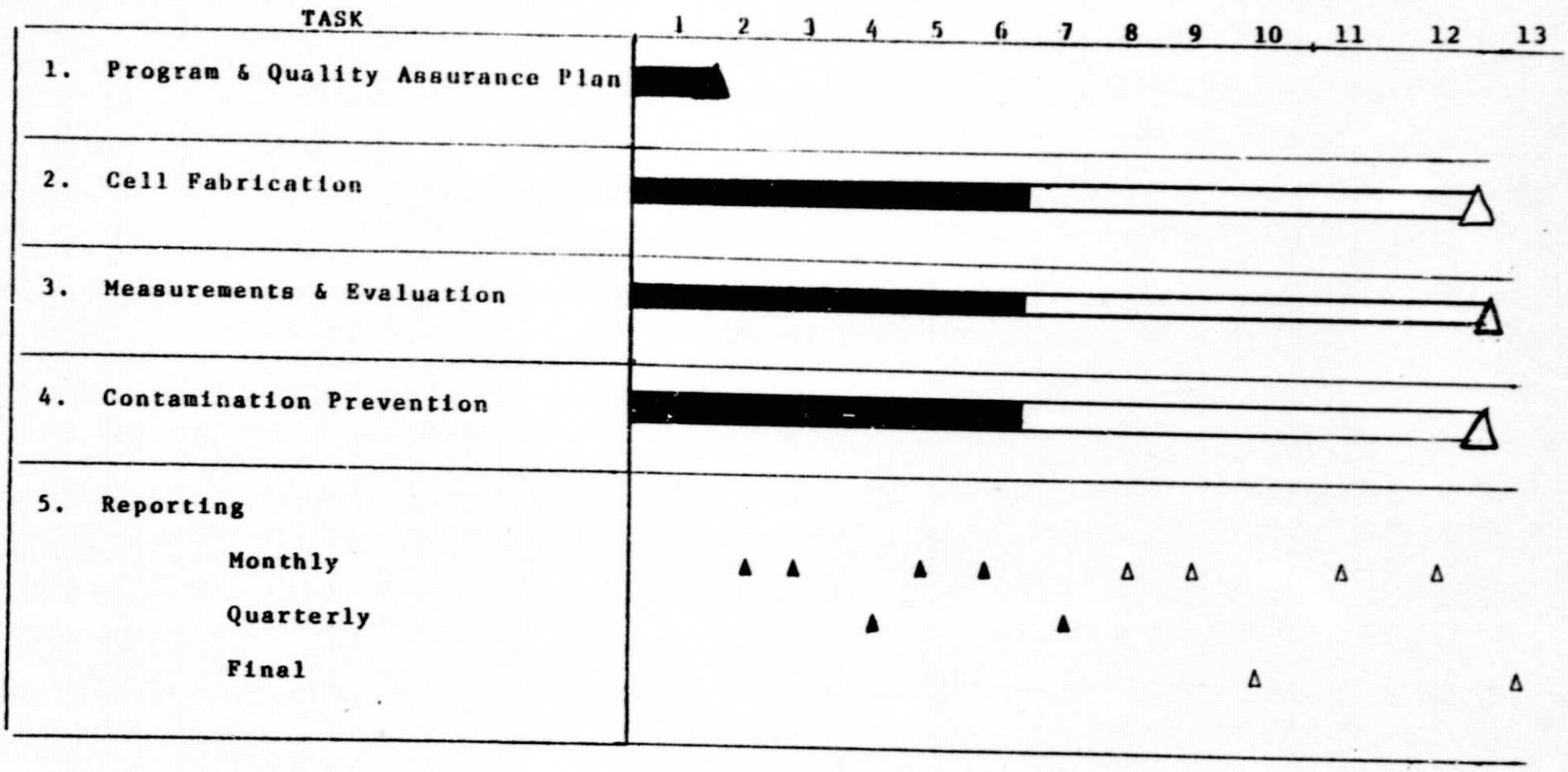

References

1. F. A. Lindholm, J. G. Fossum and E. L. Bugess, "Applications of the Super Position Principle to Solar-Cell Analysis" IEEE Trans. Electron Devices, Vol. ED-26, No.3, March 1979.

2. F. A. Lindholm, A. Neugroschel, C. T. Sah, M. P. Godlewski and H. W. Brandhorst, Jr. "A Methodology for Experimentally Based Determination of Gap Shrinkage and Effective Lifetimes in the Emitter and Base of p-n Junction Solar Cells and other p-n Junction Devices" IEEE Trans. Electron Devices, Vol. ED-24, No. 4, April 1977.

3. A. Neugroschel, F. A. Lindholm, and C. T. Sah, "A Method for Determining the Emitter and Base Lifetimes in p-n Junction Diodes," IEEE Trans. Electron Devices, Vol. ED-24, No. 6, June 1977.

4. G. Storti, S. Johnson, H. Lin and R. Armstrong, "Photovoltaic Mechanisms in Polycrystalline Thin Film Solar Cells" Second Quartly Report, DOE Contract ET-78-0-01-3413, March 1979.

5. R. H. Hopkins, et al, "Effects of Impurities and Processing on Silicon Solar Cells" Tenth Quarterly Report, DOE/JPL-954331-78/2, 1978.

6. R. H. Hopkins, et al, "Effect of Impurities and Processing on Silicon Solar Cells" Phase II Summary and Eleventh Quarterly Report, DOE/JPL-954331-78/3, 1978.

7. N. R. Draper and H. Smith, Applied Regression Analysis, John Wiley and Sons, Inc., 1966. (Typically an Analysis of Variance Table CANOVA) will contain: a) source of variation, degrees of freedom, mean square values or regression coefficients, F ratio and probability level.

Appendix A

Lot No.: V-8

Cell #	I_{sc} (mA)	V_{oc} (mV)	P_m (mW)	I_{mp} (mA)	V_{mp} (mV)	I_{sc} blue (mA)	I_{sc} red (mA)
1	150	595	70	148	500	39	84
2	150	594	66	137	480	39	83
3		Reject for poor front contact					
4		Broke					
5	151	596	68	148	500	39	84
6	154	594	67	135	475	38	87
7	153	597	72	145	506	39	86
8	153	596	70	140	505	38	87
9	153	596	73	145	510	38	81
10	151	596	72	145	510	37	86
11	152	593	72	145	510	38	86
12	149	596	72	143	510	36	80
13	152	596	72	144	510	38	86
14	150	592	65	141	474	39	84
15	152	593	70	142	500	39	85
16	151	588	66	140	500	38	85
17	150	592	68	140	500	35	87
18	150	592	70	140	500	35	82
19	150	595	70	141	510	35	87
20	147	589	66	134	505	39	85
21	150	593	65	126	500	25	88
22	151	594	70	141	525	36	86
23	149	593	69	141	500	35	86
24	151	593	69	139	500	36	86
25	149	589	70	140	510	35	87
26		Broken					
27	152	594	70	141	505	39	85
28	149	594	72	141	515	40	86

Lot No.: V-8

Cell #	I_{sc} (mA)	V_{oc} (mV)	P_m (mW)	I_{mp} (mA)	V_{mp} (mV)	I_{sc} blue (mA)	I_{sc} red (mA)
29	152	592	71	143	510	38	85
30	154	597	72	144	515	39	86
31	151	595	72	143	500	37	86
32	152	597	72	142	510	38	87
33	152	595	72	144	515	37	86
34	153	596	72	142	515	38	86
35	151	594	70	142	520	36	87
36	152	595	71	142	520	38	87
37	152	592	72	144	520	37	86
38	153	594	70	142	515	39	86
40	155	594	71	145	510	40	86
41	157	596	70	145	505	41	86
42	151	594	68	141	505	40	87
39		Reject for poor front contact					
Avg.	151.4	594.0	69.9	141.6	506.3	37.4	85.5
σ	1.88	2.17	2.21	3.92	11.27	2.62	1.70
Coef. of Var.	.012	.004	.032	.028	.022	.070	.020

Lot No.: V-10

Cell #	I_{sc} (mA)	V_{oc} (mV)	P_m (mW)	I_{mp} (mA)	V_{mp} (mV)	I_{sc} blue (mA)	I_{sc} red (mA)
1	149	592	70	141	495	40	81
2	149	592	70	140	495	39	81
3	148	582	69	140	495	39	82
4	148	592	69	139	495	41	81
5	148	589	68	138	495	39	81
6	151	593	70	140	500	39	84
7	151	593	71	139	495	38	84
8	151	592	70	140	500	38	84
9	150	591	70	140	500	38	84
10	151	593	71	142	500	40	83
11	149	587	70	142	490	38	84
12	153	594	72	144	500	38	86
13	153	594	72	145	500	39	85
14	152	591	66	135	490	38	86
15	153	591	71	142	500	38	86
16	154	594	72	142	505	39	86
17	153	594	72	142	505	38	87
18	154	585	70	142	490	39	87
19	151	592	70	140	500	38	85
20	152	591	71	144	495	36	86
21	152	592	69	140	500	37	86
22	152	593	69	140	495	37	86
23	153	592	70	143	490	38	87
24	154	593	72	145	495	39	86
25	153	593	71	142	500	38	86
26	152	592	68	140	490	38	85
27	152	594	72	144	497	38	87

Lot No.: V-10

Cell #	I_{sc} (mA)	V_{oc} (mV)	P_m (mW)	I_{mp} (mA)	V_{mp} (mV)	I_{sc} blue (mA)	I_{sc} red (mA)
28	150	592	70	140	495	36	86
29	152	591	71	142	495	38	85
30	151	590	70	141	495	37	86
31	151	590	70	141	495	38	85
32	151	589	69	141	490	38	86
33	151	592	71	140	500	37	86
34	151	590	71	143	495	39	85
35	152	591	70	142	495	39	85
36	151	590	70	142	490	37	86
37	151	592	70	140	500	37	87
Avg.	151.3	591.5	70.2	141.2	496.3	38.2	85.0
σ	1.63	1.97	1.29	1.98	4.15	1.05	1.80
Coef. of Var.	.011	.003	.018	.014	.008	.027	.021

Appendix B

Lot No.: E-1 Test Cells (111) CP

Cell #	I_{sc} (mA)	V_{oc} (mV)	P_m (mW)	I_{mp} (mA)	V_{mp} (mV)	I_{sc} blue (mA)	I_{sc} red (mA)
T1 s	.142	569	59	128	460	35	80
T2 s	.146	574	60	127	475	36	83
T3 s	145	575	63	132	475	36	81
T4 s		REJECT					
T5 c	141	575	61	127	480	38	78
(5 cells)							
AVG	143.5	573.3	60.8	128.5	472.5	36.3	80.5
σ	2.38	2.87	1.71	2.38	8.66	1.26	2.08
Coef. Var	.017	.005	.028	.019	.018	.035	.026

Lot N.: [illegible] Test C[illegible](1-1-1)

Cell #	I_{sc} (mA)	V_{oc} (mV)	P_m (mW)	I_{mp} (mA)	V_{mp} (mV)	I_{sc} blue (mA)	I_{sc} red (mA
$T1_s$	144	578	64	134	480	41	74
$T2_s$	142	575	61	127	480	39	75
$T3_s$	146	577	65	135	480	40	77
$T4_s$	139	580	67	139	485	40	80
$T5_c$	145	579	66	136	485	41	76
$T6_c$	144	578	65	134	485	40	77
$T7_c$	146	577	64	133	475	40	78
$T8_c$	144	579	65	134	485	40	75
$T9_c$	144	579	66	136	485	41	75
$T10_t$	145	578	66	137	480	41	76
$T11_t$	144	580	66	136	485	43	75
$T12_t$	145	577	64	133	480	40	77
$T13_t$	146	579	62	134	465	41	77
13 cells)							
Avg.	144.2	578.2	64.7	134.5	480.8	40.5	76.3
σ	1.91	1.41	1.70	2.82	5.72	.97	1.60
Coef. Var.	.013	.002	.026	.021	.012	.024	.021

Lot N.: E-3 - Test (111) CP

Cell #	I_{sc} (mA)	V_{oc} (mV)	P_m (mW)	I_{mp} (mA)	V_{mp} (mV)	I_{sc} blue (mA)	I_{sc} red (m
T1 s	136	611	62	118	530	37	73
T2 s	134	606	54	108	500	38	70
T3 c	138	609	56	111	505	38	74
T4 c	133	609	56	111	505	37	70
T5 c	132	610	60	116	515	37	70
T6 c	133	612	62	121	515	37	71
T7 c	132	611	62	117	525	37	69
T8 c	135	610	61	117	520	36	72
T9 c	136	614	65	123	530	37	73
T10 c	131	605	51	101	505	36	70
T11 c	136	614	63	120	525	37	73
11 cells							
AVG	134.2	610.1	59.3	114.8	515.9	37.0	71.4
σ	2.18	2.84	4.36	6.48	10.9	0.63	1.69
Coef.Var	.016	.005	.073	.056	.021	.017	.024

Lot. No.: E-4- Test (111) CP

Cell #	I_{sc} (mA)	V_{oc} (mV)	P_m (mW)	I_{mp} (mA)	V_{mp} (mV)	I_{sc} blue (mA)	I_{sc} red (mA
1. s	140	612	66	128	515	39	73
2. s	140	611	65	126	510	40	72
3. s	139	611	65	127	510	38	73
4. s	139	609	60	121	505	39	72
5.c	139	611	66	127	520	38	74
6. c	138	610	65	126	515	38	72
7. c	140	611	67	130	515	38	75
8. c	138	610	64	124	520	38	72
9. c	138	578	60	124	485	37	73
10. c		REJECT					
11	------ Broken -----						
*12 t		REJECT					
13 t	138	602	62	122	505	37	73
cell	#12 is 1.3 cm x 2.cm						
All 10 cells avg	138.9	606.5	64.0	125.5	510.0	38.2	72.9
σ	0.88	10.41	2.49	2.76	10.27	0.92	0.99
cv	.006	.017	.039	.022	.020	.024	.014
seed							
cells avg	139.5	610.8	64.0	125.5	510.0	39.0	72.5
σ	0.58	1.26	2.71	3.11	4.08	0.82	0.58
cv	.004	.002	.042	.025	.008	.021	0.008

Lot N.: Lot-5 Test (1-1-1) CP

Cell #	I_{sc} (mA)	V_{oc} (mV)	P_m (mW)	I_{mp} (mA)	V_{mp} (mV)	I_{sc} blue (mA)	I_{sc} red
1s	139	566	62	131	475	38	72
2s	140	566	62	130	475	39	73
*3s		----------REJECT----------					
**4s		----------REJECT----------					
5c	134	562	60	126	475	38	70
6c	137	562	53	113	475	38	72
7c	134	561	58	123	470	37	69
8		----------BROKEN----------					
9c	134	511	58	123	475	38	69
10t	127	553	47	106	460	34	67
11t	134	560	56	118	470	38	69
12t	134	562	60	125	475	39	68
13t	133	559	58	123	470	40	66
*	1x2cm						
**	missing corner						
10 cells							
AVG.	134.6	561.2	57.6	121.8	472.0	37.9	69.5
σ	3.60	3.68	4.06	7.64	4.83	1.60	2.27
Coef. Var.	.027	.007	.070	.063	.010	.042	.033